Atmos. Chem. Phys., 8, 6137–6145, 2008
www.atmos-chem-phys.net/8/6137/2008/

Atmospheric Chemistry and Physics

SO_2 Retrieval from SCIAMACHY using the Weighting Function DOAS (WFDOAS) technique: comparison with Standard DOAS retrieval

C. Lee[1,*], **A. Richter**[1], **M. Weber**[1], **and J. P. Burrows**[1]

[1]Institute of Environmental Physics and Remote Sensing, University of Bremen, Bremen, Germany
[*]now at: Department of Physics and Atmospheric Science, Dalhousie University, Halifax, Canada

Received: 8 April 2008 – Published in Atmos. Chem. Phys. Discuss.: 5 June 2008
Revised: 21 August 2008 – Accepted: 11 September 2008 – Published: 22 October 2008

Abstract. Atmospheric SO_2 can be measured by remote sensing of scattered sunlight from space, using its unique absorption features in the ultraviolet region. However, the sensitivity of the SO_2 measurement depends critically on spectral interference, surface albedo and varies with wavelength as Rayleigh scattering increases at shorter wavelengths. The Weighting Function Differential Optical Absorption Spectroscopy (WFDOAS) method was used to pinpoint these problems and improve the retrieval. The Ring spectra included in the WFDOAS fit were determined as a function of total ozone column density, solar zenith angle, surface albedo, and effective scene altitude. The WFDOAS SO_2 retrieval from SCIAMACHY (Scanning Imaging Absorption Spectrometer for Atmospheric Chartography) data onboard the ENVISAT satellite are presented here and compared to those of the Standard DOAS (SDOAS) method for cases of background conditions and volcanic eruption. The study demonstrates the problems in the SO_2 retrieval with SDOAS, such as the positive offsets over remote (clean) regions and the negative offsets at high solar zenith angles and high ozone, could be attributed to imperfect correction for the varying ozone dependence of the Ring effect and could be solved by the WFDOAS approach.

1 Introduction

Sulfur dioxide (SO_2) plays an important role in the atmospheric sulfur cycle, in the formation of new aerosols, and the modification of existing aerosols (Chin and Jacob, 1996; Berglen et al., 2004). There is concern about the impact of SO_2 on global climate through the formation and modification of aerosols and their effects on the radiation balance of the atmosphere (Intergovernmental Panel on Climate Change (IPCC), 2001; Myhre et al., 2004), as well as on ecosystems and human health. SO_2 is released into the atmosphere as a result of both anthropogenic activities and natural (e.g., volcanic) phenomena (Seinfeld and Pandis, 1998; Finlayson-Pitts and Pitts, 2000).

Anthropogenic emissions of SO_2 occur predominantly from fossil fuel combustion at the continental surface and chemical conversion and loss processes take place during transport (Tan et al., 2002; Koike et al., 2003; Guttikunda et al., 2005). Volcanoes are an important natural source of various atmospheric trace gases, in particular SO_2. Volcanic eruptions inject gases and particles into the atmosphere, leading to tropospheric and stratospheric aerosol formation. Highly explosive volcanic events affect climate on time scales of months to years (McCormic et al., 1995; Robock, 2000). Neither the anthropogenic SO_2 flux nor the flux from volcanic emissions is easy to determine precisely, on account of the dispersion of anthropogenic sources over large areas. Since volcanic eruptions and their emissions are sporadic and intermittent and often occur in uninhabited regions, it is difficult to assess the amount and size of the emissions from volcanoes. Satellite remote sensing measurements are well-suited to overcome these difficulties.

SO_2 observations from space was first performed using Total Ozone Mapping Spectrometer (TOMS) (Krueger, 1983), and later using other satellite instruments such as the Global Ozone Monitoring Experiment (GOME), Scanning Imaging Absorption Spectrometer for Atmsopheric Chartography (SCIAMACHY) and Ozone Measurement Instrument (OMI) (e.g., Krueger et al., 1995; Eisinger and Burrows, 1998; Afe et al., 2004; Carn et al., 2004; Khokhar et al.,

Correspondence to: C. Lee
(cklee79@gmail.com)

Published by Copernicus Publications on behalf of the European Geosciences Union.

2005; Thomas et al. 2005; Krotkov et al., 2006; Richter et al., 2006; Carn et al., 2007; Yang et al., 2007; Krotkov et al., 2008). Modification and development of algorithms used to retrieve data from satellite observations have been of primary interest. The satellite remote sensing approach associated with the Differential Optical Absorption Spectroscopy (DOAS) technique (Platt, 1994) has been successfully employed for measurements of atmospheric trace gases on global and regional scales (e.g., Chance, 1998; Eisinger et al., 1998; Wagner et al., 1998; Martin et al., 2002; Palmer et al., 2003; Afe et al., 2004; Richter et al., 2005; Wittrock et al., 2006; Lee et al., 2008).

However, the Standard DOAS (called SDOAS here) retrieval of SO_2 from satellite measurements in the UV wavelength range is in difficulties for e.g., a spectral interference (for details see Sect. 2). To improve the SO_2 retrieval, SO_2 retrievals using the Weighting Function Differential Optical Absorption Spectroscopy (WFDOAS) method was applied here. In the following, we present problems with the SDOAS retrieval and the concept of the WFDOAS retrieval. Section 2 describes SCIAMACHY SO_2 retrievals with SDOAS and WFDOAS. In Sect. 3, the results from the two techniques are compared and the effect from different Ring parameterizations is evaluated. In this study we concentrated on selected scenarios with anthropogenic and volcanic emissions as well as background conditions in December 2006. The airmass factor (AMF) calculation to convert the slant columns (SC) to vertical columns (VC) is not covered here, but will be considered in future work.

1.1 Problems with the Standard DOAS retrieval

The Standard DOAS retrieval of SO_2 from measurements of GOME (Burrows et al., 1999) and SCIAMACHY (Bovensmann et al., 1999) works well over areas with strongly enhanced SO_2 after volcanic eruptions (Khokhar et al., 2005; Richter et al., 2006). These plumes can be easily identified and tracked with high accuracy. Also, areas suffering from strong SO_2 pollution can be identified at least in monthly averages. However, there are a number of problems with the SO_2 data that need to be solved for a better exploitation of the satellite measurements:

1. There is an offset in the SO_2 slant columns that leads to positive values over remote (clean) regions. This offset varies over time and with latitude. Up to now, the approach used to account for this is to subtract the values over a clean reference sector, which greatly reduces the problem at low and middle latitudes but often fails at higher latitudes. The origin of the offset is unknown but it depends on the exact choice of fitting window and cross-sections, indicating a spectral interference problem.
2. At high latitudes/high ozone levels, the retrieved SO_2 columns are negative as a result of interference with ozone and its temperature dependence. The O_3 AMF varies significantly with wavelength and these variations are correlated with the O_3 bands. In addition, the sensitivity of SO_2 retrievals also varies with wavelength as Rayleigh scattering increases at shorter wavelengths.
3. Over elevated areas, the SO_2 column is smaller and after offset correction often negative. This is the case over the Himalaya, the Andes, and the Alps but also over the Western part of the US. It is speculated that this is related to interference with Ring effect, the "filling-in" of solar Fraunhofer lines in the scattered light, but no clear conclusion has been drawn so far (Van Roozendael et al., 2002).
4. Over bright surfaces, such as Greenland or the South Pole, often unrealistically large SO_2 columns are observed.
5. The overall scatter in the SO_2 values is large, in particular for SCIAMACHY measurements. The Southern Atlantic Anomaly has a large impact in an area covering large parts of South America and the South Atlantic reaching the African coast. Higher particle fluxes in this region result in random isolated spikes in SO_2. This can be improved by extending the SO_2 fitting window to the UV, but this reduces sensitivity to boundary layer SO_2.

1.2 Concept of the Weighting Function DOAS retrieval

In an attempt to solve at least some of the problems with the SDOAS retrieval, SO_2 retrievals using the WFDOAS method were performed and results compared to those from SDOAS. The WFDOAS is distinguished from the SDOAS by the use of wavelength-dependent weighting functions of ozone and temperature, which describe the relative radiance change due to a vertical profile change. The WFDOAS method has been first demonstrated to be applicable to retrievals of trace gas columns in the near infrared region of SCIAMACHY (Buchwitz et al., 2000). It is also being used for direct retrieval of vertical O_3 amounts (Coldewey-Egbers et al., 2005; Weber et al., 2005; Bracher et al., 2005). It is distinct from the SDOAS by the use of wavelength-dependent weighting functions, which describe the relative radiance change due to a vertical profile change. The weighting function for the ozone column change is obtained by integrating vertically the altitude dependent weighting function. Such an approach is particularly suited to DOAS retrievals of strong absorbers like ozone in the UV spectral region. In addition, the effect of rotational Raman scattering (Ring effect) is accounted for by using a pre-calculated data base of Raman reference spectra which is tabulated as a function of ozone column density, solar zenith angle, surface albedo, and altitude (Coldwey-Egbers et al., 2005). Here, we limit the weighting functions

Table 1. Specifications of SO_2 retrievals for SCIAMACHY data using Weighting Function DOAS (WFDOAS) and Standard DOAS (SDOAS) techniques.

	Wavelength range, nm	Polynomial order	Cross-sections included in the fit
SDOAS	315–327	4	SO_2 at 295 K (Vandaele et al., 1994), O_3 at 223 K and 243 K (Bogumil et al., 2003), Ring spectrum (Voutas et al., 1998), Undersampling correction, Polarization dependency
WFDOAS	315–327	3	SO_2 at 295 K (Vandaele et al., 1994), O_3 weighting function, Temperature weighting function, BrO at 228 K (Wahner et al., 1988), Online calculated Ring spectrum

to ozone and temperature, and SO_2 is only fitted as an additional absorber, which means that SO_2 cross-section is fitted to obtain the slant column amount. The WFDOAS SO_2 retrievals are still expected to be superior to those of SDOAS as the strong interference by ozone and Ring effect is optimally handled.

2 Measurement data and retrieval methods

2.1 SCIAMACHY instrument

SCIAMACHY is one of ten instruments onboard ESA's Environmental Satellite (ENVISAT) which was launched into a sun-synchronous orbit in March 2002. The SCIAMACHY instrument is an 8 channel grating spectrometer measuring in nadir, limb, and occultation (both solar and lunar) viewing geometries (Bovensmann et al., 1999). SCIAMACHY covers the spectral region from 220 to 2400 nm with a spectral resolution of 0.25 nm in the UV, 0.4 nm in the visible and less in the NIR. In these wavelength regions several trace gases were detected in the past (e.g., Afe et al., 2004; Buchwitz et al., 2005; Richter et al., 2005; Wittrock et al., 2006). The size of the nadir ground-pixels depends on wavelength range and solar elevation and can be as small as $30\times30\,km^2$. The SO_2 column retrieval is done using spectra from Channel 2 (310–405 nm) in nadir viewing geometry.

2.2 Standard DOAS retrieval

The SDOAS method has been used for the SO_2 retrieval for GOME and SCIAMACHY in previous studies (Eisinger and Burrows, 1998; Afe et al., 2004; Khokhar et al., 2005; Richter et al., 2006; Lee et al., 2008). In this work, the wavelength range of 315–327 nm is used for the SO_2 DOAS fit as the differential absorptions are large and interference by other species (apart from ozone) is small. In addition to the SO_2 cross-section (Vandaele et al., 1994), two ozone cross-sections (Bogumil et al., 2003), a synthetic Ring spectrum (Vountas et al., 1998), an undersampling correction (Chance, 1998), and the polarization dependency of the SCIAMACHY instrument are included in the fit. The specifications of the SDOAS SO_2 retrieval are summarized in Table 1. Daily solar irradiation measurements taken with the ASM diffuser are used as background spectrum. In the comparison with the WFDOAS retrieval, the reference sector method (RSM, for details see Martin et al., 2002; Richter and Burrows, 2002) is applied to remove a meridional offset in the SDOAS SO_2 SC by subtracting the columns of a presumably SO_2 free reference sector over a remote area, which were taken on the same day at the same latitude in the 180° E–230° E longitudinal range.

2.3 Weighting Function DOAS retrieval

Weighting Functions are the derivative of the radiation field with respect to the atmospheric parameters and they are used in the retrieval of strongly absorbing species (Rozanov et al., 1998). The WFDOAS algorithm was originally applied to the retrieval of vertical O_3 amounts from GOME and SCIAMACHY data in the wavelength region of 326.6–335.0 nm (Coldewey-Egbers et al., 2005). Here we extend it for the SO_2 retrieval by changing the wavelength region and adding SO_2 as an additional absorber (see Table 1).

Figure 1 shows the WFDOAS algorithm scheme used for the SO_2 retrieval in this work. The radiative transfer model, SCIATRAN 2.0 (Rozanov et al., 1997) is integrated into the iterative retrieval scheme. In earlier versions the radiative transfer quantities were read from look-up-tables. In the WFDOAS retrieval the measured atmospheric optical depth is approximated by a Taylor expansion around the reference intensity. A third order polynomial P_i is added to account for all broad band contributions from surface albedo and aerosol. The Ring spectrum, the BrO absorption cross-section as well as the SO_2 absorption cross-section (for all of which slant column fitting is applied) are included in the WFDOAS fitting. The optical depth equation can be written as follows (Coldewey-Egbers et al., 2005):

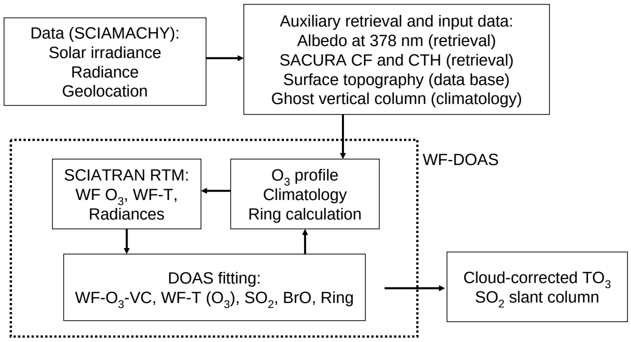

Fig. 1. Scheme of the WFDOAS algorithm for SO_2 retrieval from SCIAMACHY data. The radiative transfer model, SCIATRAN 2.0 was incorporated to calculate the modelled radiance and weighting functions. CF and CTH indicate cloud fraction and cloud-top-height from the SACURA algorithm (Kohkanovsky et al., 2006), respectively.

$$\begin{aligned}\ln I_i^{\mathrm{mea}}(V^t,\vec{b^t}) \approx{}& \ln I_i^{\mathrm{mod}}(\bar{V},\bar{\vec{b}}) + \frac{\partial \ln I_i^{\mathrm{mod}}}{\partial V}\Big|_{\bar{V}} \times (\hat{V}-\bar{V}) \\ &+ \frac{\partial \ln I_i^{\mathrm{mod}}}{\partial V}\Big|_{\bar{T}} \times (\hat{T}-\bar{T}) \\ &+ SCD_{\mathrm{SO_2}} \times \sigma_{i,\mathrm{SO_2}} \\ &+ SCD_{\mathrm{BrO}} \times \sigma_{i,\mathrm{BrO}} \\ &+ SCD_{\mathrm{Ring}} \times \sigma_{i,\mathrm{Ring}} \\ &+ P_i \end{aligned} \quad (1)$$

where I^{mea} is the measured intensity and I^{mod} is the sun-normalized reference intensity as provided by SCIATRAN 2.0. Index t denotes the true atmospheric state. The entire right-hand side of the equation (excluding the reference intensity) has to be adjusted to the measured intensity (left-hand side) for all spectral points (index i) simultaneously. $\bar{V}$ is the reference ozone column corresponding to the reference intensity, and $\bar{T}$ is the reference surface temperature. $\hat{V}$ and $\hat{T}$ denote the corresponding fit parameters. The specifications for the WFDOAS SO_2 retrieval are shown in Table 1.

In the WFDOAS fitting, the atmospheric scenario which most closely matches the O_3 vertical column derived from the IUP climatology (Lamsal et al., 2004) is selected using linear interpolation between effective albedo, relative azimuth angle and geo-location data. A reference spectrum to account for the Ring effect was calculated online as a function of total ozone column including ozone profile shape, solar zenith angle, surface albedo, altitude, and viewing geometries using SCIATRAN 2.0, but no interpolation was done (Weber et al., 2007). Ozone and temperature profiles are taken from the IUP climatology (Lamsal et al., 2004) which contains different profile shapes for three latitude belts (tropics, middle and high latitudes in each hemisphere) and two seasons (winter/spring and summer/fall) as a function of the total ozone column. The Ring spectrum σ_{Ring} has been approximated as follows:

$$\sigma_{\mathrm{Ring}} = \frac{I_0^{rrs}}{I_0} \exp\left(\frac{\tau_{\mathrm{O_3}}^{v}}{\cos(\theta_0)}\left(1-\frac{\sigma_{\mathrm{O_3}}^{rrs}}{\sigma_{\mathrm{O_3}}}\right)\right) \quad (2)$$

where the index rrs indicates the Raman smoothed quantity, I_0 the solar irradiance, σ_{O_3} ozone cross-section, θ_0 the solar zenith angle, and $\tau_{\mathrm{O_3}}^{v}$ the vertical optical density of O_3 (Weber et al., 2007).

The ozone and temperature weighting functions and modeled radiances (reference intensity) are calculated as a function of solar zenith angle, line of sight, relative azimuth angle, surface height, and effective albedo using SCIATRAN 2.0. The DOAS fitting utilized a non-linear least square method, including wavelength shifts and squeeze for the nadir measurement spectrum to make the direct comparison between measured and modeled radiances (Coldewey-Egbers et al., 2005; Weber et al., 2005). After DOAS fitting the retrieved ozone column was compared with that of the reference scenario. The fit is repeated with an updated set of weighting functions until the change in retrieved value is below a convergence limit (see Fig. 1).

2.4 OMI SO_2 data

In addition, OMI SO_2 SC data converted from the publicly released Planetary Boundary Layer (PBL) OMI SO_2 Level 2 VC products (http://daac.gsfc.nasa.gov/) are added for comparison with the WFDOAS SCIAMACHY SO_2. The OMI SO_2 SC data are retrieved with the Band Residual Difference (BRD) algorithm (Krotkov et al., 2006, 2008). In this retrieval, the "sliding median" empirical correction is used to reduce any cross-track and meridional biases, which subtracts a median residual for a sliding group of SO_2 free pixels covering ±15° latitude along the orbit track from each spectral band and cross-track position (Yang et al., 2007; Krotkov et al., 2008). There is cloud screening in these publicly released PBL SO_2 data using the removal of all measurements with surface reflectivity larger than 30%. The OMI PBL SO_2 VCs were converted back to SC using the original constant AMF of 0.36.

3 Results of the retrievals

3.1 Ring effect in the WFDOAS SO_2 retrieval

Figure 2 shows the WFDOAS fitting results of two cases: one using the online Ring spectrum calculation (ORSC) as described in Sect. 2.3 and the other using just a single Ring spectrum (Vountas et al., 1998), which is based on one standard ozone profile and only depends on the solar zenith angle. The spectra representing background conditions as shown in Fig. 2 were taken in the 60° E and 100° E longitudinal region on 30 November 2005 (SCIAMACHY orbit

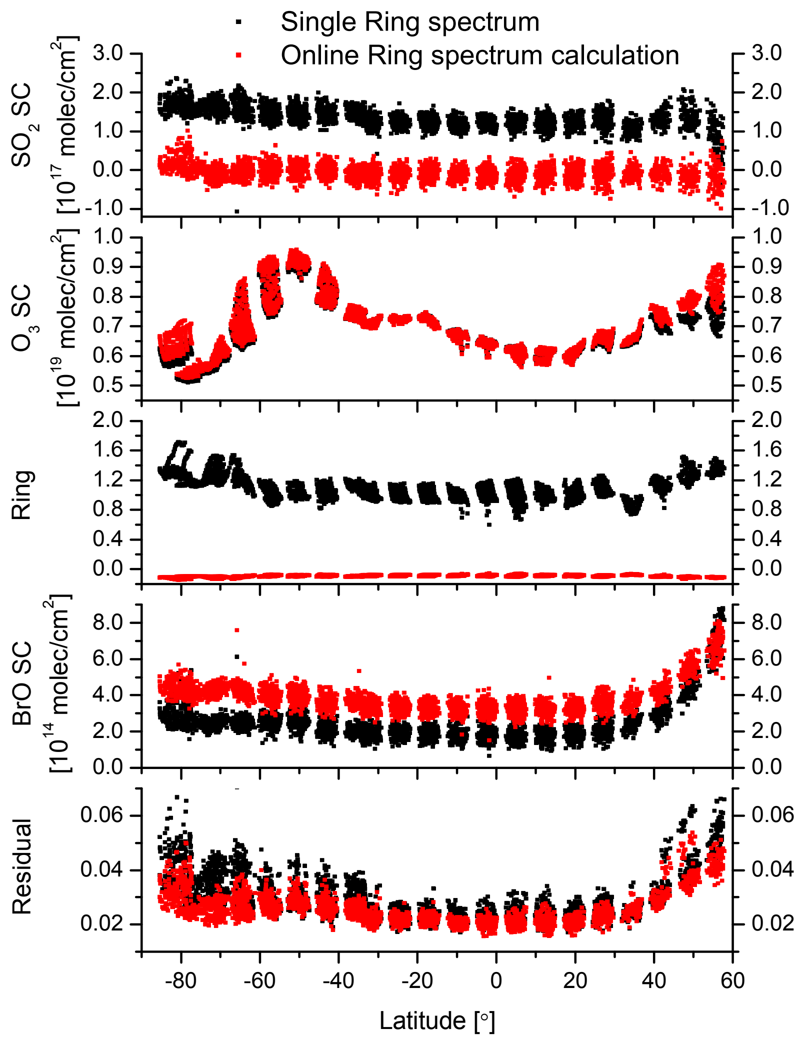

Fig. 2. Results of WFDOAS retrieval: (red dots) retrievals integrating the online Ring spectrum calculation (ORSC) and (black dots) incorporating a single Ring spectrum (Vountas et al., 1998). The spectra were taken in the 60° E and 100° E longitudinal region on 30 November 2005 (SCIAMACHY orbit no. 19611). Residuals are peak-to-peak values.

no. 19611). As seen in the top panel of Fig. 2, the WFDOAS retrieval including a single Ring spectrum has positive offsets over the tropics and mid latitudes. These offsets decrease slightly at higher latitudes, while they are decreasing and even reaching negative values at high latitudes in the SDOAS retrievals (see Fig. 3a). These offsets over the tropics and mid latitudes are not present when using the ORSC. Even the slightly decreasing offset over higher latitudes is removed when using the ORSC. O_3 columns at higher latitudes are slightly lower compared to those obtained by using a single Ring spectrum. Also important, the fit residual decreased in the WFDOAS retrieval using the ORSC. It seems that depending on how the Ring effect is calculated, it may be responsible for positive offsets in the SO_2 SCs.

3.2 Comparison of WFDOAS with SDOAS results

Figure 3 shows the SO_2 slant columns retrieved with WFDOAS and SDOAS for one orbit with background conditions (a), where SO_2 is expected to be below the detection limit, and another orbit covering a volcanic eruption (b). The orbit used for the background condition is the same as that shown in Fig. 2. Volcanic eruption spectra were obtained in the 20° W–30° E longitudinal region on 2 December 2006 (SCIAMACHY orbit no. 24868). The OMI SO_2 SC data corresponding to geo-locations of SCIAMACHY data measured on the same day are plotted in Fig. 3.

As shown in Fig. 3a, the SDOAS results have positive offsets over tropical and mid latitude areas, and are decreasing and even reaching negative values at higher latitudes under background conditions. SO_2 levels in the SDOAS retrieval of volcanic emissions are overestimated compared to that

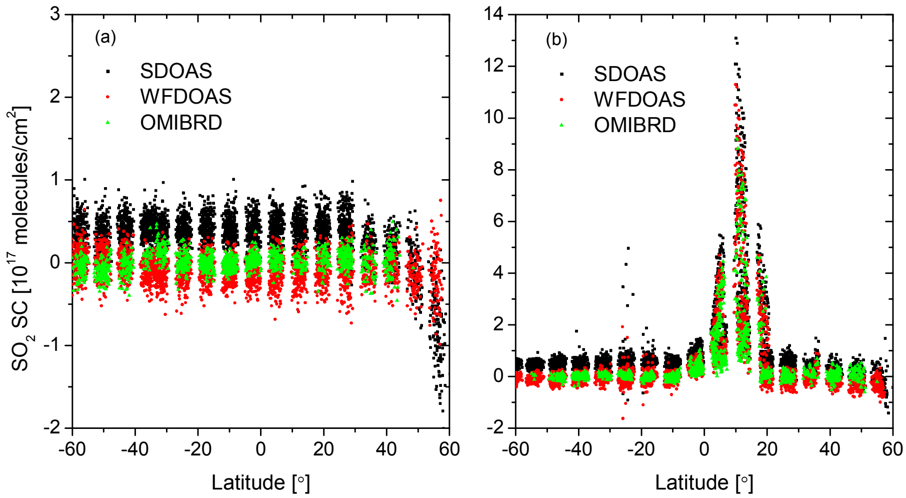

Fig. 3. SO_2 slant columns retrieved by WFDOAS (red dots) and SDOAS (black dots) methods in the cases of remote background conditions **(a)** and a volcanic eruption **(b)**. The spectra for background conditions were taken in the 60° E and 100° E longitudinal region on 30 November 2005 (SCIAMACHY orbit no. 19611, see also Fig. 2). Spectra of the volcanic eruption (near and around Nyamuragira volcano in Congo, erupted on 27 November 2006) were obtained in the 20° W–30° E longitudinal region on 2 December 2006 (SCIAMACHY orbit no. 24868). For the comparison of SCIAMACHY SO_2 slant columns (SC) with OMI SO_2 SC (yellowish green dots) are added, which are retrieved with the Band Residual Difference (BRD) algorithm (Krotkov et al., 2006, 2008).

WFDOAS retrieval (see Fig. 3b). The differences between SDOAS and WFDOAS are not a result from different polynomial degrees and absorbers (e.g. BrO in WFDOAS only, ETA and undersampling only in SDOAS), summarized in Table 1. The polynomial degrees and BrO do not have affect on SO_2 slant columns in the WFDOAS retrieval, not contributing the differences between SDOAS and WFDOAS retrievals. However, both the third order polynomial and BrO in the fit lead to less fit residual in the WFDOAS retrieval.

The constant and latitudinal offsets in the retrieved SO_2 SC have also been reported in previous SDOAS SO_2 retrieval studies (e.g., Khokhar et al., 2005; Richter et al., 2006). SO_2 shows clear absorption features in the retrieval wavelength range of 315–327 nm. In this wavelength range ozone absorption is, however, strong and interferes with SO_2. Negative SO_2 SC values may occur, when the varying ozone dependence of the Ring effect is not properly accounted for, particularly, with increasing slant O_3 absorption at higher SZAs (see Fig. 3a). The levels of OMI SO_2 are likely to be in the agreement with the WFDOAS SCIAMACHY SO_2 and show less scatter compared to the SDOAS and WFDOAS SCIAMACHY SO_2. The OMI SO2 SCs are stable over tropic and mid-latitudes but have relatively larger scatter at larger SZA. Note that the "sliding median" empirical correction and cloud-screening are used in the OMI SO_2 retrieval and the number of OMI SO_2 data points is less than SCIAMACHY SC data.

Monthly mean SO_2 slant column maps from December 2006 are shown in Fig. 4 for the WFDOAS retrieval, the SDOAS retrieval, the SDOAS retrieval after applying the reference sector (RSM) correction, and the BRD OMI retrieval. The WFDOAS results show less meridional offsets, compared to those of the SDOAS retrieval, while it shows slightly higher offsets compared to the RSM-applied SDOAS results. The meridional offset over low and mid latitude areas are completely removed in the RSM-corrected SDOAS retrieval, but not in some areas at high latitudes where the instrument took measurements at large solar zenith angles.

The seven day mean of BRD OMI SO_2 SC from 1 to 7 December 2006 is presented in Fig. 4. Its background level is in the agreement with the RSM-corrected SDOAS retrieval. Both SCIAMACHY and OMI observed volcanic SO_2 signals around Nyamuragira volcano in Congo (erupted on 27 November 2006), as also seen in Fig. 3b. There are some breaks in these volcanic signals in the SCIAMACHY data because it takes turns about recording signals in nadir and limb modes. In monthly mean data the volcanic SO_2 signals observed from the OMI instrument for December 2006 are lower than those from SCIAMACHY. The difference in monthly average volcanic SO_2 amounts can be explained by sampling effect (the average OMI SC on volcanic plumes should be lower than the SCIAMACHY SC as the OMI samples each pixel every day and the SCIAMACHY needs 6 days to acquire a contiguous global map).

4 Conclusions

The crucial role of SO_2 in the oxidation capacity of the atmosphere and the assessment of natural radiative forcing of atmospheric sulfate aerosols are well known. The development

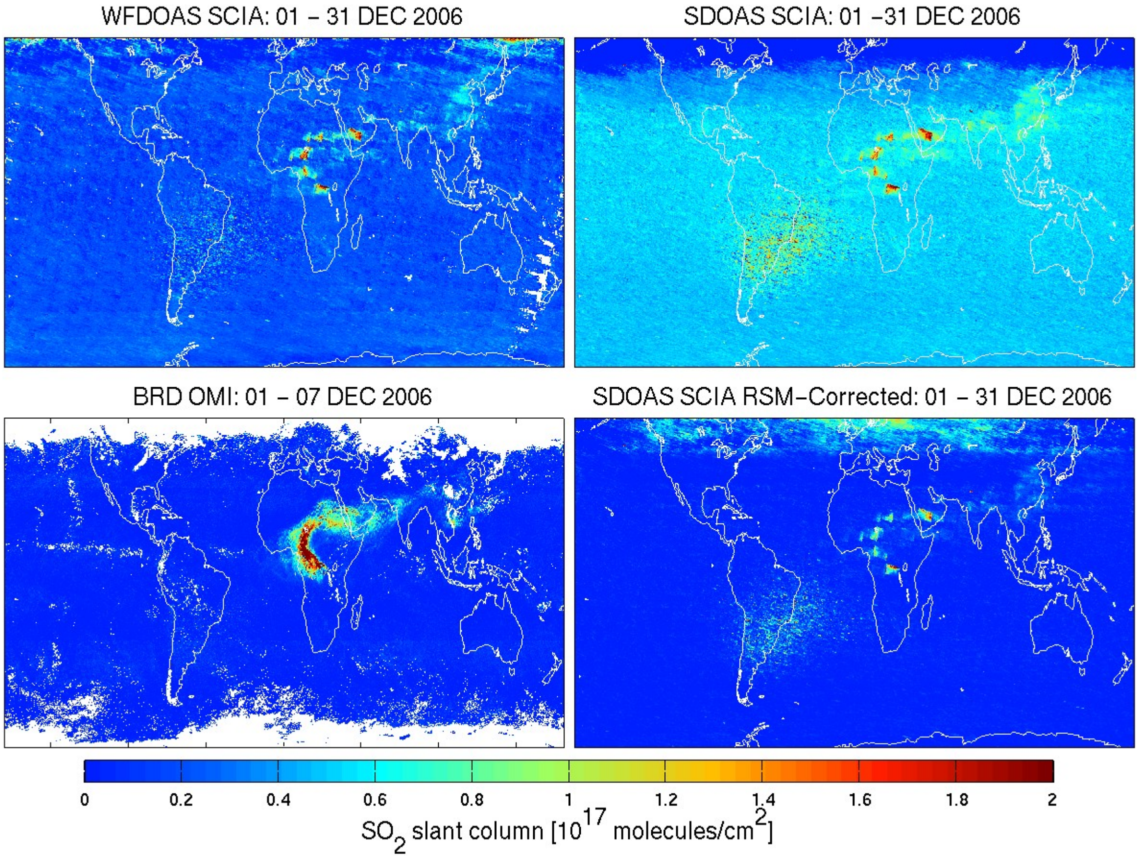

Fig. 4. Global maps of SO_2 slant columns averaged over December 2006. The panels show SO_2 slant columns from the WFDOAS retrieval (top left), the SDOAS retrieval (top right), the RSM-corrected SDOAS retrieval (bottom right), and the OMI BRD algorithm (bottom left). In the area of the Southern Atlantic Anomaly (SAA), large scatter in WFDOAS and SDOAS SCIAMACHY SO_2 results from exposure of the instrument to radiation and particles. RSM: Reference sector method (Martin et al., 2002; Richter and Burrows, 2002). There are the open areas in WFDOAS retrievals due to no SACURA data and in the BRD OMI retrievals due to cloud-screening.

of robust control strategies to reduce SO_2 levels in the atmosphere requires more precise evaluation of the amount of natural and anthropogenic SO_2 from space. Satellite measurements of SO_2 can help to better identify and quantify the amount of natural and anthropogenic emissions of SO_2 and their transport and conversion to sulfate aerosols in the atmosphere. However, the SO_2 slant column retrieval in the UV spectral region is quite challenging due to strong interference with absorption by ozone, which can produce positive offsets over remote (clean) regions, negative offsets at high latitudes and in region with high ozone, and smaller values over elevated areas, which after correction with the reference sector method often become negative.

Some of these problems in the SDOAS retrieval of SO_2 can be overcome by using the WFDOAS approach which improves the fit because

1. the wavelength dependence of the ozone airmass factor is accounted for by using weighting functions, and
2. the treatment of the Ring effect is improved when obtained from a complex data base which depends on ozone column, reflectivity, and SZA, which appears to be the most crucial factor in the SO_2 retrieval using the WFDOAS technique.

The ability of WFDOAS retrieval as an alternative method for SDOAS methods was demonstrated here. Monitoring of volcanic emission and ambient air pollution is important in terms of global SO_2 budget and ambient air quality. The WFDOAS retrieval showed clearly volcanic emissions (e.g., near and around Nyamuragira volcano in Congo, erupted on 27 November 2006) and ambient air pollution of SO_2 (e.g., over northeastern China). The current version of the WFDOAS retrieval is computationally expensive (~4 h per one orbit data on our local machine compared to several minutes in the SDOAS retrieval). It may be considerably sped up by use of look-up-tables. Up to now, it is suitable mainly for case studies.

Slant column fitting errors (100–200% relative errors) in WFDOAS retrieval are at levels similar to those in SDOAS retrievals and could be associated with the intrinsic measurement noise of SCIAMACHY. The elevated fitting errors are related to low radiances measured by SCIAMACHY at shorter wavelengths and high solar zenith angle (or high ozone). The measurement of low radiances leads to the uncertainties in SO_2 retrievals.

The measurements of SO_2 emissions (in particular volcanic SO_2 emissions) from space suffer from sparse temporal and spatial coverage of current satellite sensors but also from clouds in the troposphere. However, satellite measurements of SO_2 are a crucial step forward for real time monitoring of air pollution change on a global scale, and can provide information for near real-time application and forecasting such as hazard warning and air-quality monitoring.

Acknowledgements. This work was supported by the Korea Research Foundation Grant funded by the Korean Government (MOEHRD) (KRF-2006-214-D00085). The SCIAMACHY data were obtained from Institute of Environmental Physics and Remote Sensing, University of Bremen, Germany.

Edited by: U. Platt

References

Afe, O. T., Richter, A., Sierk, B., Wittrock, F., and Burrows, J. P.: BrO emission from volcanoes: a survey using GOME and SCIAMACHY measurements, Geophys. Res. Lett., 31, L24113, doi:10.1029/2004GL020994, 2004.

Berglen, T. F., Berntsen, T. K., Isaksen, I. S. A., and Sundet, J. K.: A global model of the coupled sulfur/oxidant chemistry in the troposphere: the sulfur cycle, J. Geophys. Res., 109, D19310, doi:10.1029/2003JD003948, 2004.

Bogumil, K., Orphal, J., Homann, T., Voigt, S., Spietz, P., Fleischmann, O. C., Vogel, A., Hartmann, M., Bovensmann, H., Frerik, J., and Burrows, J. P.: Measurements of molecular absorption spectra with the SCIAMACHY Pre-Flight Model: Instrument characterization and reference data for atmospheric remote sensing in the 230-2380 nm region, J. Photoch. Photobio. A, 157, 167–184. 2003.

Bovensmann, H., Burrows, J. P., Buchwitz, M., Frerick, J., Noel, S., Rozanov, V. V., Chance, K. V., and Goede, A. H. P.: SCIAMACHY-Mission objectives and measurement modes, J. Atmos. Sci., 56, 127–150, 1999.

Bracher, A., Lamsal, L. N., Weber, M., Bramstedt, K., Coldewey-Egbers, M., and Burrows, J. P.: Global satellite validation of SCIAMACHY O_3 columns with GOME WFDOAS, Atmos. Chem. Phys., 5, 2357–2368, 2005, http://www.atmos-chem-phys.net/5/2357/2005/.

Buchwitz, M., de Beek, R., Burrows, J. P., Bovensmann, H., Warneke, T., Notholt, J., Meirink, J. F., Goede, A. P. H., Bergamaschi, P., Körner, S., Heimann, M., and Schulz, A.: Atmospheric methane and carbon dioxide from SCIAMACHY satellite data: initial comparison with chemistry and transport models, Atmos. Chem. Phys., 5, 941–962, 2005, http://www.atmos-chem-phys.net/5/941/2005/.

Buchwitz, M., Rozanov, V. V., and Burrows, J. P.: A near-infrared optimized DOAS method for the fast global retrieval of atmospheric CH_4, CO, CO_2, H_2O, and N_2O total column amounts from SCIAMACHY Envisat-1 nadir radiances, J. Geophys. Res., 105, 15 231–15 245, 2000.

Burrows, J. P, Weber, M., Buchwitz, M., Rozanov, V. V., Ladstädter-Weissenmayer, A., Richter, A., de Beek, R., Hoogen, R., Bramstedt, K., Eichmann, K.-U., Eisinger, M., and Perner, D.: The Global Ozone Monitoring Experiment (GOME): Mission concept and first scientific results, J. Atmos. Sci., 56, 151–175, 1999.

Carn, S. A., Krotkov, N. A., Gray, M. A., and Krueger, A. J.: Fire at Iraqi sulfur plant emits SO_2 clouds detected by Earth Probe TOMS, Geophys. Res. Lett., 31, L19105, doi:10.1029/2004GL020719, 2004.

Carn, S. A., Krueger, A. J., Krotkov, N. A., Yang, K., and Levelt, P. F.: Sulfur dioxide emissions from Peruvian copper smelters detected by the Ozone Monitoring Instrument, Geophys. Res. Lett., 34, L09801, doi:10.1029/2006GL029020, 2007.

Chance, K.: Analysis of BrO Measurements from the Global Ozone Monitoring Experiment, Geophys. Res. Lett., 25, 3335–3338, 1998.

Chin, M. and Jacob, D. J.: Anthropogenic and natural contributions to tropospheric sulfate: a global model analysis, J. Geophys. Res., 101, 18 691–18 669, 1996.

Coldewey-Egbers, M., Weber, M., Lamsal, L. N., de Beek, R., Buchwitz, M., and Burrows, J. P.: Total ozone retrieval from GOME UV spectral data using the weighting function DOAS approach, Atmos. Chem. Phys., 5, 1015–1025, 2005, http://www.atmos-chem-phys.net/5/1015/2005/.

Eisinger, M. and Burrows, J. P.: Tropospheric sulfur dioxide observed by the ERS-2 GOME instrument, Geophys. Res. Lett., 25, 4177–4180, 1998.

Finlayson-Pitts, B. J. and Pitts, J. N.: Chemistry of the Upper and Lower Atmosphere, Academic Press, San Diego, CA, USA, 2000.

Guttikunda, S. K., Tang, Y., Carmichael, G. R., Kurata, G., Pan, L., Streets, D. G., Woo, J.-H., Thongboonchoo, N., and Fried, A.: Impacts of Asian megacity emissions on regional air quality during spring 2001, J. Geophys. Res., 110, D20301, doi:10.1029/2004JD004921, 2005.

Khokhar, M. F., Frankenberg, C., Van Roozendael, M., Beirle, S., Kühl, S., Richter, A., Platt, U., and Wagner, T.: Satellite observation of atmospheric SO_2 from volcanic eruptions during the time-period of 1996–2002, Adv. Space Res., 36, 879–887, 2005.

Kokhanovsky, A. A., von Hoyningen-Huene, W., Rozanov, V. V., Noël, S., Gerilowski, K., Bovensmann, H., Bramstedt, K., Buchwitz, M., and Burrows, J. P.: The semianalytical cloud retrieval algorithm for SCIAMACHY II. The application to MERIS and SCIAMACHY data, Atmos. Chem. Phys., 6, 4129–4136, 2006, http://www.atmos-chem-phys.net/6/4129/2006/.

Koike, M., Kondo, Y., Kita, K., Takegawa, N., Masui, Y., Miyazaki, Y., Ko, M. W., Weinheimer, A. J., Flocke, F., Weber, R. J., Thornton, D. C., Sachse, G. W., Vay, S. A., Blake, D. R., Streets, D. G., Eisele, F. L., Sandholm, S. T., Singh, H. B., and Talbot, R. W.: Export of anthropogenic reactive nitrogen and sulfur compounds from the East Asia region in spring, J. Geophy. Res., 108, D20, doi:10.1029/2002JD003284, 8789, 2003.

Krotkov, N. A., Carn, S. A., Krueger, A. J., Bhartia, P. K., and Yang, K.: Band residual difference algorithm for retrieval of SO_2 from the Aura Ozone Monitoring Instrument (OMI), IEEE T. Geosci. Remote, 44, 1259–1266, 2006.

Krotkov, N. A, McClure, B., Dickerson, R. R., Carn, S. A., Can, L., Bhartia, P. K., Yang, K., Krueger, A. J., Li, Z., Levelt, P. F., Chen, H., Wang, P., Daren, L.: Validation of SO_2 retrievals from the Ozone Monitoring Instrument (OMI) over NE China, J. Geophys.Res., D16S40, doi:10.1029/2007JD008818, 2008.

Krueger, A.: Sighting of El Chichon sulfur dioxide clouds with the Nimbus 7 total ozone mapping spectrometer, Science, 220, 1377–1379, 1983.

Krueger, A., Walter, L., Bhartia, P., Schnetzler, C., Krotkov, N., Sprod, I., and Bluth, G.: Volcanic sulfur dioxide measurements from the total ozone mapping spectrometer instruments, J. Geophys. Res., 100, 14 057–14 076, 1995.

Lamsal, L. N., Weber, M., Tellmann, S., and Burrows, J. P.: Ozone column classified climatology of ozone and temperature profiles based on ozone sondes and satellite data, J. Geophy. Res., 109, D20304, doi:10.1029/2004JD004680, 2004.

Lee, C., Richter, A., Burrows, J. P., Lee, H., Kim, Y. J., Lee, Y. G., and Choi, B. C.: Impact of transport of sulfur dioxide from the Asian continent on the air quality over Korea during May 2005, Atmos. Environ., doi:10.1016/j.atmosenv.2007.11.006, 2008.

Martin, R. V., Chance, K., Jacob, D. J., Kurosu, T. P., Spurr, R. J. D., Bucsela, E., Gleason, J. F., Palmer, P. I., Bey, I., Fiore, A. M., Li, Q., Yantosca, R. M., and Koelemeijer, R. B. A.: An improved retrieval of tropospheric nitrogen dioxide from GOME, J. Geophy. Res., 107, D20, 4437, doi:10.1029/2001JD001027, 2002.

McCormick, M. P., Thomason, L. W., and Trepte, C. R: Atmospheric effects of the Mt Pinatubo eruption, Nature, 373, 399–404, 1995.

Myhre, G., Berglen, T. F., Myhre, C. E. L., and Isaksen, I. S. A.: The radiative effect of the anthropogenic influence on the stratospheric sulfate aerosol layer, Tellus B, 56, doi:10.1111/j.1600-0889.2004.00106.x, 294–299, 2004.

Palmer, P. I., Jacob, D. J., Fiore, A. M., Martin, R. V., Chance, K., and Kurosu, T. P.: Mapping isoprene emissions over North America using formaldehyde column observations from space, J. Geophy. Res., 108, D5, 4180, doi:10.1029/2002JD002153, 2003.

Platt, U.: Differential optical absorption spectroscopy (DOAS), in: Monitoring by Spectroscopic Techniques, Wiley & Sons, New York, USA, 27–84, 1994.

Richter, A. and Burrows, J. P.: Tropospheric NO_2 from GOME measurements, Adv., Space Res., 29, 1673–1683, 2002.

Richter, A., Burrows, J. P., Nüß, H., Granier, C., and Niemeier, U.: Increase in tropospheric nitrogen dioxide over China observed from space, Nature, 437, 129–132, 2005.

Richter, A., Wittrock, F., and Burrows, J. P.: SO_2 Measurements with SCIAMACHY, in Proc. Atmospheric Science Conference, 8–12 May 2006, ESRIN, Frascati, ESA publication SP-628, 2006.

Robock, A.: Volcanic eruption and climate, Rev. Geophys., 38, 191–219, 2000.

Rozanov, V. V., Kurosu, T., and Burrows, J. P.: Retrieval of atmospheric constituents in the UV-visible: A new quasi-analytical approach for the calculation of weighting functions, J. Quant. Spectrosc. Ra., 60, 277–299, 1998.

Rozanov, V. V., Diebel, D., Spurr, R. J. D., and Burrows, J. P: GOMETRAN: A radiative transfer model for the satellite project GOME – The plane parallel version, J. Geophys. Res., 102, 16 683–16 695, 1997.

Seinfeld, J. H. and Pandis, S. N.: Atmospheric Chemistry and Physics, John Wiley & Sons, New York, USA, 1998.

Tan, Q., Huang, Y., and Chameides, W. L.: Budget and export of anthropogenic SOx from East Asia during continental outflow condition, J. Geophy. Res., 107, D13, 4167,doi:10.1029/2001JD000769, 2002.

Thomas, W., Erbertseder, T., Ruppert, T., Van Roozendael, M., Verdebout, J., Balis, D., Meleti, C., and Zerefos, C.: On the retrieval of volcanic sufur dioxide emissions from GOME backscatter measurements, J. Atmos. Chem., 50, 295–320, 2005.

Vandaele, A. C., Simon, P. C., Guilmot, J. M., Carleer, M., and Colin, R.: SO_2 absorption cross section measurement in the UV using a Fourier transform spectrometer, J. Geophy. Res., 99, 25 599–25 605, 1994.

Van Roozendael, M., Soevijanta, V., Fayt, C., and Lamvert, J.-C.: Investigation of DOAS issues affecting the accuracy of the GDP version 3.0 total ozone product, in: ERS-2 GOME GDP 3.0 Implementation and Delta Validation, ERSE-DTEX-EOAD-TN-02-0006, ESA/ESRIN, Frascati, Italy, 97–129, 2002.

Vountas, M., Rozanov, V. V., and Burrows, J. P.: Ring effect: Impact of rotational Raman scattering on radiative transfer in earth's atmosphere, J. Quant. Spectrosc. Ra., 60, 943–961, 1998.

Wagner, T. and Platt, U.: Satellite mapping of enhanced BrO concentrations in the troposphere, Nature, 395, 486-490, 1998.

Wahner, A., Ravishankara, A. R., Sander, S. P., and Friedl, R. R.: Absorption cross section of BrO between 312 and 385 nm at 298 and 223 K, Chem. Phys. Lett., 152, 507–512, 1988.

Weber, M., Lamsal, L. N., Coldewey-Egbers, M., Bramstedt, K., and Burrows, J. P.: Pole-to-pole validation of GOME WFDOAS total ozone with groundbased data, Atmos. Chem. Phys., 5, 1341–1355, 2005, http://www.atmos-chem-phys.net/5/1341/2005/.

Weber, M., Lamsal, L. N., and Burrows, J. P.: Improved SCIAMACHY total ozone retrieval: Steps towards homogenizing long-term total ozone datasets from GOME, SCIAMACHY, and GOME2, The 2007 ESA ENVISAT Symposium, Montreux, Switzerland, 23–27 April 2007, 2007.

Wittrock, F., Richter, A., Oetjen, H., Burrows, J. P., Kanakidou, M., Myriokefalitakis, S., Volkamer, R., Beirle, S., Platt, U., and Wagner, T.: Simultaneous global observations of glyoxal and formaldehyde from space, Geophys. Res. Lett., 33, L16804, doi:10.1029/2006GL026310, 2006.

Yang, K., Krotkov, N. A., Krueger, A. J., Carn, S. A., Bhartia, P. K., and Levelt, P. F.: Retrieval of large volcanic SO2 columns from the Aura Ozone Monitoring Instrument: Comparison and limitations, J. Geophy. Res., 112, D24S43, doi:10.1029/2007JD008825, 2007.